Available online at www.sciencedirect.com
ScienceDirect
International Journal of Mass Spectrometry 269 (2008) 177–186
International Journal of Mass Spectrometry
www.elsevier.com/locate/ijms

Theoretical investigation on reactivity of Ag and Au atoms toward CS_2 in gas phase

Xin Wang [a,b,*], Ling Yang [a], An-Min Tian [a], Ning-Bew Wong [c,**]

[a] *Faculty of Chemistry, Sichuan University, Chengdu 610064, China*
[b] *State Key Laboratory of Biotherapy, Sichuan University, Chengdu 610041, China*
[c] *Department of Biology and Chemistry, City University of Hong Kong, Kowloon, Hong Kong*

Received 6 June 2007; received in revised form 2 October 2007; accepted 9 October 2007
Available online 16 October 2007

Abstract

The reaction mechanisms of Ag and Au atoms with CS_2 on both doublet and quartet potential energy surfaces (PESs) have been investigated using UBPW91 and UCCSD(T) methods. The two studied reactions proceed via a similar insertion–elimination mechanism instead of a direct abstract mechanism. The reaction $Ag + CS_2 \rightarrow SAgCS$ is endothermic by about 21.0 kcal/mol. But another reaction $Au + CS_2 \rightarrow SAuCS$ is slightly exothermic by about 8.8 kcal/mol, which is different from the previous theoretical prediction. In the overall reactions, the rate-determining step is found to be the C–S bond cleavage step with a high-activation barrier of about 40 kcal/mol. The calculated vibration frequencies are in good agreement with the experiment values and show that the BPW91 method is very good for the calculation of small molecules containing Ag and Au. The reactivity of the two atoms toward CS_2 is compared with those of the first-row transition-metal atoms. The present study provides a detailed picture of the C–S bond activation and cleavage in carbon disulfide mediated by second and the third row transition-metal atoms Ag and Au.

Keywords: Quantum chemistry calculation; Metal sulfide; Reaction mechanism; Activation barrier

1. Introduction

The chemistry of transition-metals sulfides has been an active field of both theoretical and experimental researches due to its important role in industry and biology systems [1–4]. In industrial areas, metal sulfides are widely used in lubrication, energy storage, and catalysis [1,2]. In many biological systems, sulfur coordination is very significant where they appear [3,4]. Carbon disulfide, CS_2, an important sulfur-transfer species, can react with metal atoms or ions to form metal sulfides. It has also recently been considered as a sulfur source for preparing thin layers of semiconductor materials [5]. In this light, reactions of the transition-metal atoms or cations with CS_2 have been extensively studied by experimentalists and theoreticians in recent years [6–15]. In experimental investigations, the groups of Schwarz and Armentrout reported their collaborative works on gas-phase reactions of atomic metal cations with CS_2 [6–13]. In these works, Fourier transform ion cyclotron resonance (FTICR) mass spectrometry and guided ion beam (GIB) mass spectrometry were used to study the reactions of CS_2 with ionic species Sc^+ [6], Ti^+ [6], V^+ [7–9], Cr^+ [10], Mn^+ [10], Fe^+ [11], Co^+ [11], Ni^+ [12], Cu^+ [12], Zn^+ [12], Mo^+ [9], Y^+ [13], Zr^+ [13], and Nb^+ [13]. Most recently, Böhme and coworkers [14] reported an extensive experiment survey on 46 atomic metal cations with CS_2 using an inductively coupled plasma/selected-ion flow tube (ICP/SIFT) tandem mass spectrometer. The investigations demonstrate that CS_2 shows a high reactivity toward atomic cations. In the theoretical approaches, Rue et al. [8] have investigated the reaction of $V^+ + CS_2$ using B3LYP and CASSCF methods. The surface-crossing behavior of the reaction was discussed and compared with experimental results. Jiang and Zhang [15] provided a detailed theoretical insight into the quartet and sextet potential energy surfaces of the $[Fe, C, S_2]^+$. Their calculations indicate that the reaction proceeds via an insertion–elimination mechanism instead of a direct abstract mechanism.

* Corresponding author at: Faculty of Chemistry, Sichuan University, Chengdu 610064, China. Tel.: +86 28 85412800; fax: +86 28 85412800.
** Corresponding author.
E-mail addresses: wangxin@scu.edu.cn (X. Wang), bhnbwong@cityu.edu.hk (N.-B. Wong).

1387-3806/$ – see front matter © 2007 Elsevier B.V. All rights reserved.
doi:10.1016/j.ijms.2007.10.002

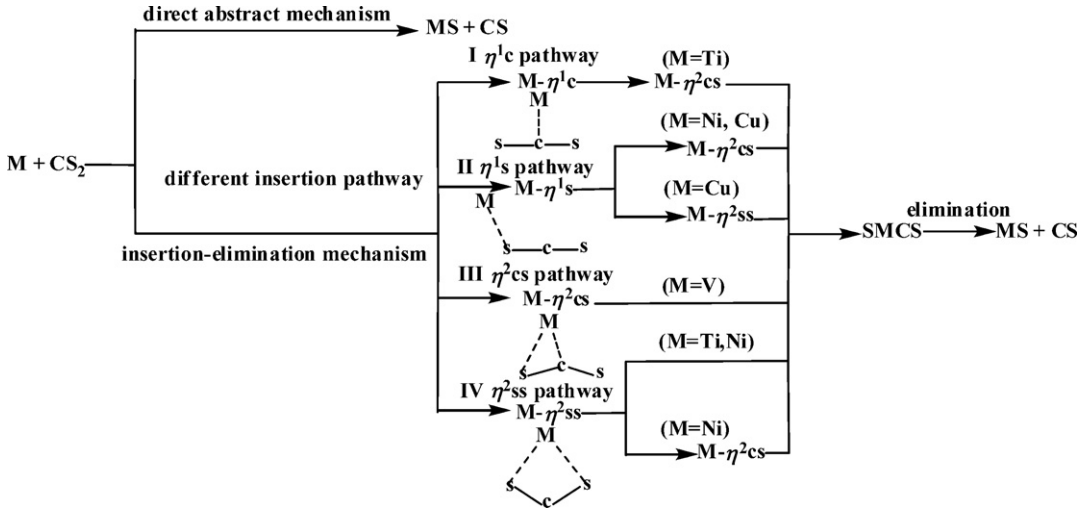

Scheme 1. Summary for the diverse pathways of reactions $M + CS_2 \rightarrow MS + CS$.

Compared with the fruitful studies on reactivities of metal cations toward CS_2, the reaction of neutral transition-metal atoms with CS_2 is relatively unexplored. Andrews and coworkers reported their study of laser-ablated Co [16], Ni [16], Cu [16], Sc [17], Y [17] and La [17] atom reactions with CS_2 using matrix isolation infrared spectroscopy. In theoretical works, the reaction mechanism between first-row transition-metal atoms, V [18], Ni [19], Ti [19], and Cu [20], and CS_2 have been investigated with density function theory (DFT). These researches indicate that the reactions of the first-row transition-metal atoms with CS_2 can proceed in a similar insertion–elimination mechanism. An insertion product SMCS yields through various intermediate coordination complexes. The reactions proceed via different mechanisms. The diverse insertion pathways can be classified according to different initial intermediate complexes, which are summarized in Scheme 1.

One may notice that the studies on the reaction of the second and third row transition-metal atoms with CS_2 are relatively rare. Recently, Zeng et al. [21] reported a matrix isolation IR study on the reactions of ablated Ag and Au atoms with CS_2. An insertion product ^{2}SMCS formed under photolysis condition was detected. They also performed a DFT calculation to identify the observed complexes and insertion products (M–η^1s and SMCS, where M means a metal). In quite recent investigation on reaction of Ag^+ and Au^+ cations with CS_2 [14], the exclusive CS_2 addition was observed with Ag^+ and the monosulfide cation of Au^+ was detected to be produced with only a branching ratio of 1% and the main products of the reaction are the $Au^+(CS_2)n$ clusters. These researches show that the Ag and Au atom are more active than their cations to react with CS_2. Clearly, the details of the two titled reactions are interesting. The investigations on the reaction mechanism will provide a detailed insight on reactivities of the second and the third transition-metal atoms toward CS_2. In previous theoretical studies on reaction of metal atoms and CS_2, only first-row transition-metal atoms have been reported. Thus, a theoretical investigation on the mechanisms of the two reactions is valuable. To our best knowledge, this has not been done so far. Through DFT calculations carried out on the complexes and insertion products of the two reactions [21], the insertion pathways and active barrier heights of the two reactions are still unknown. Since the ground states of Cu, Ag, and Au atoms have the same $(n-1)d^{10}ns^1$ electronic configuration it is also interesting to compare the reactivities and insertion pathways of the three metal atoms in the same group. In this paper, we will use DFT calculations to explore the mechanisms of the reactions $M + CS_2 \rightarrow MS + CS$ (M = Ag and Au) in details. We hope that our study will provide a deeper insight on the reaction of the second and third row transition-metal atoms with CS_2.

2. Computational details

The ground doublet and quartet potential energy surfaces (PESs) of the two reactions have been explored. The DFT is employed with the Becke's [22] exchange functional and the Perdew et al. [23] correlation functional (BPW91). For metal atoms Ag and Au, the relativistic effective core potential (ECP) [24] is employed in all BPW91 calculations. The basis set for Ag and Au is a modified LANL2DZ double-ζ basis set plus an f-type polarization function [25], in which the two 4p functions of the standard LANL2DZ have been replaced by the optimized 4p functions from Couty and Hall [26]. The standard 6–311+G(d) basis set is used for the rest of the atoms. All together, the basis set described above is called basis set I (abbreviated as BI). The geometries of reactants, intermediates, transition states, and insertion products are fully optimized using unrestricted BPW91 (UBPW91) method with BI described above. For each species, the harmonic vibrational frequencies are calculated to obtain the zero-point energies (ZPE) and verified whether there is a minimum or a transition state (TS) on its PES. Intrinsic reaction coordinate (IRC) analysis [27] is performed to identify the minimum energy path (MEP) from a transition state to the corresponding local minimum in a step size of 0.1 $(amu)^{1/2}$ Bohr.

To obtain more accurate energetics of potential energy profiles, we also perform single-point UCCSD(T) energy cal-

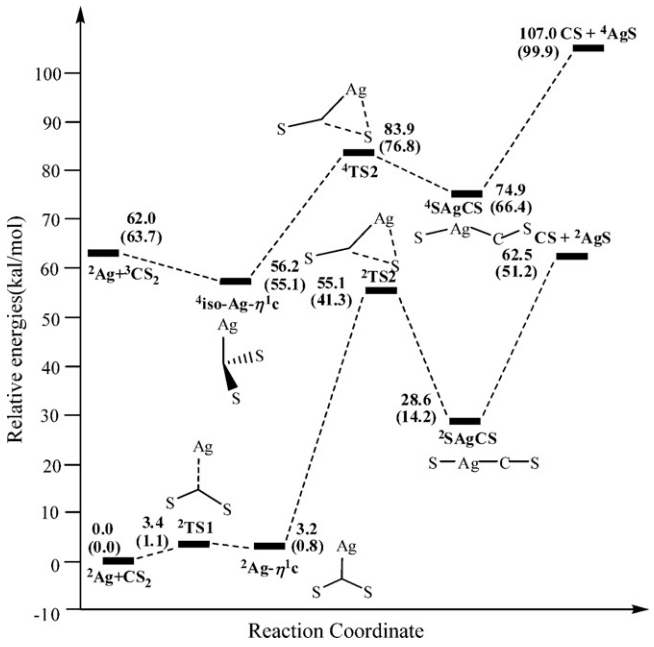

Fig. 1. Potential energy profiles of the doublet and quartet pathways of the reaction Ag + CS_2 → AgS + CS at the UBPW91/BI level. The ZPE corrections are included in the relative energies. The relative energies at the UCCSD(T)/BII//UBPW91/BI level are in parentheses. The ZPE-corrected energy of ^{2}Ag + ^{1}CS_2 is taken to be zero.

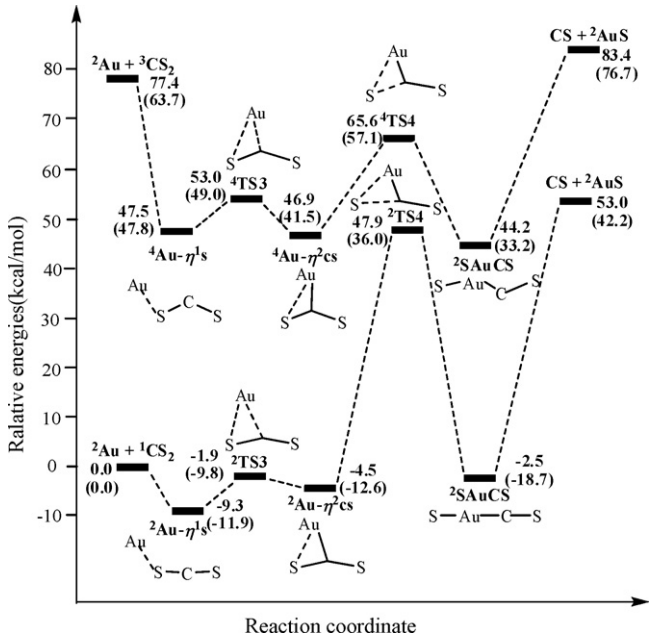

Fig. 3. Potential energy profiles of doublet and quartet pathways of the reaction Au + CS_2 → AuS + CS at the UBPW91/BI level. The ZPE corrections are included in the relative energies. The relative energies at the UCCSD(T)/BII//UBPW91/BI level are in parentheses. The ZPE-corrected energy of ^{2}Au + ^{1}CS_2 is taken to be zero.

culations using a larger basis set BII. The basis BII consists of an ECP on metal atom with the modified LANL2DZ basis set and the standard 6–311+G(3df) basis set on all other atom. Before the single-point energy calculations, stability tests of wave functions are always carried out to ensure that the lowest energy solution in the SCF procedure is found. The natural bond orbital (NBO) analysis [28] is also carried out to calculate the NBO charge at the UBPW91/BI level. All calculations have been performed with the Gaussian 03 package of programs[29].

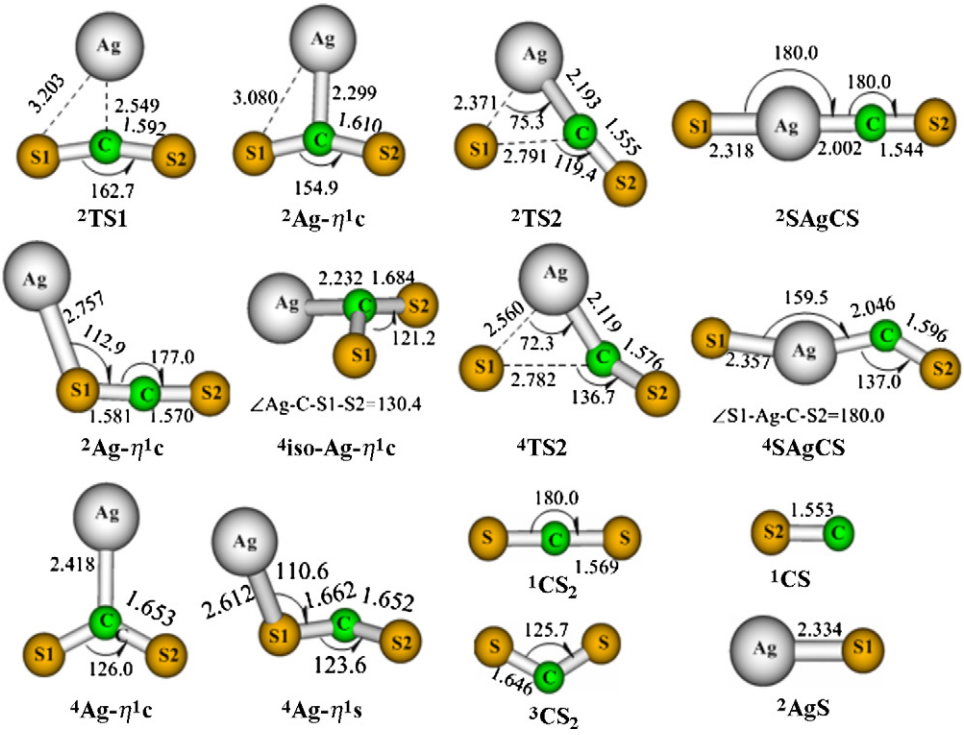

Fig. 2. Optimized geometries of the various stationary points on the Ag + CS_2 doublet and quartet PESs (distances in angstroms, angles in degrees).

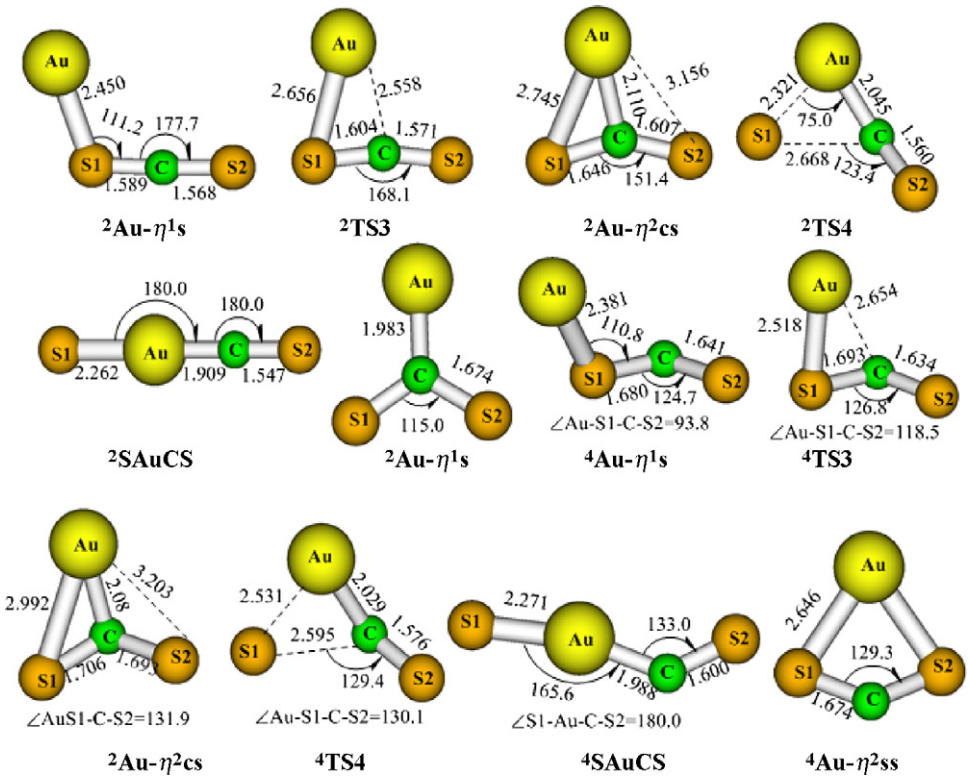

Fig. 4. Optimized geometries of the various stationary points on the Au + CS_2 doublet and quartet PESs (distances in angstroms, angles in degrees).

3. Results and discussion

In Figs. 1 and 2, the potential energy profiles of the two reactions are shown, respectively. The optimized structures of stationary points are displayed in Figs. 3 and 4. The calculated the dissociation energies (D_o), C–S bond length, and atomization energies are listed in Table 1.The calculated total energies, zero-point energies (ZPE), and relative energies for all species are collected in Tables 2 and 3. The corresponding harmonic vibrational frequencies and infrared intensities are shown in Table 4. In Tables 5 and 6, spin densities and natural charges on atoms of some species are listed, respectively.

3.1. Assessment of the calculation methods

In the past 10 years, DFT method has been widely used to calculate systems containing transition metals and established as the most useful theoretical tool for quantum chemistry calculations [30,31]. In previous theoretical researches on reactions of metal atoms and CS_2 [18–20], hybrid B3LYP function is chosen. However, for molecules containing the coinage metals such as Ag and Au, calculated energies are very sensitive to DFT functionals [32,33], we have to choose the functional very carefully. Legge et al. [32] reported the DFT calculations for typical Cu-, Ag-, Au-containing molecules with various DFT functionals and recommended that the combination BPW91/LANL2DZ could be used for noble-metal systems because of its accuracy and reliability. To find a reliable functional for describing the current M + CS_2 (M = Ag and Au) systems, we calculated the dissociation energies (D_o) of the small species (AgO, AgS, AuO and AuS). Relative calculation errors in the calculated values of D_o are compared with experimental data [34] and the results are shown in Table 1. In Scheme 2, the error bars of different functional are drawn. We also optimized the structures of CS_2 molecule with different functional and calculated its atomization energies. As shown in Table 1, the calculated C–S bond lengths are all in good agreement with the experimental result and the BLYP yield the most accurate atomization energies. Compared the theoretical D_o with experimental data, we can find that the pure and hybrids DFT methods are all superior to the MP2 method, and within the former, all the errors of the pure are smaller than that of the hybrids. The BPW91 method performs marginally better than the B3LYP method and the others. The

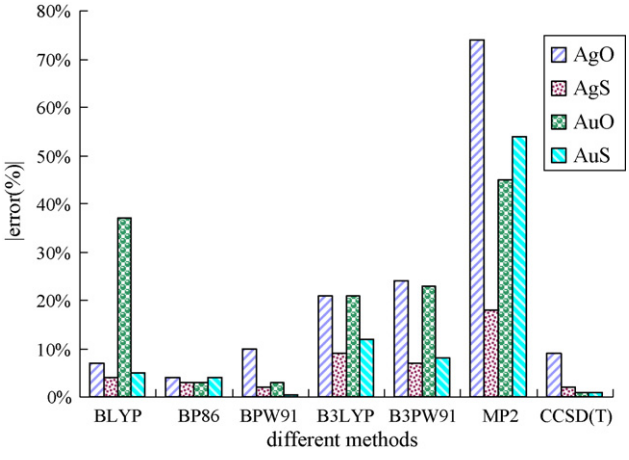

Scheme 2. The error bars of D_o using different theoretical methods.

Table 1
Dissociation energies D_o (eV), errors (%), C–S bond lengths of CS_2, and atomization energies of CS_2 calculated using different methods and basis set BI

Species	Experimental[a]	BLYP		BP86		BPW91		B3LYP		B3PW91		MP2		CCSD(T)[b]	
	D_o (eV)	eV	%	eV	%	eV	%	eV	%	eV	%	eV	%	eV	%
AgO(^{2}P)	2.29	2.13	−7	2.19	−4	2.05	−10	1.81	−21	1.75	−24	0.66	−74	2.08	−9
AgS(^{2}P)	2.21	2.12	−4	2.28	3	2.17	−2	2.01	−9	2.06	−7	1.82	−18	2.17	−2
AuO(^{2}P)	2.33	3.19	37	2.40	3	2.25	−3	1.83	−21	1.79	−23	3.37	45	2.31	−1
AuS(^{2}P)	2.59	2.46	−5	2.69	4	2.58	0	2.28	−12	2.37	−8	3.99	54	2.56	−1

Species	Experimental[c], r (Å)	BLYP	BP86	BPW91	B3LYP	B3PW91	MP2
CS_2	1.556	1.575	1.570	1.569	1.561	1.557	1.562

Species	Experimental[d], E (kcal mol^{-1})	BLYP	BP86	BPW91	B3LYP	B3PW91	MP2
CS_2	273.2	273.9	287.3	282.6	265.0	271.0	298.8

[a] Experimental values, all from Ref. [34].
[b] The D_o was computed at the CCSD(T)/BII//BPW91/BI level. The calculated value of AgO, AgS, AuO, and AuS at the CCSD(T)/BI//BPW91/BI level are 1.31, 1.85, 3.52, and 2.20 eV, respectively.
[c] Experimental value from Ref. [38].
[d] Atomization energies. The experiment determinations are obtained on the basis of the experimental heats of formation of atoms and CS_2 molecules from Ref. [39].

CCSD(T) single-point calculations are also performed with two basis sets, 6–311+G(d) and 6–311+G(3df). As shown in Table 1, the error for calculated D_o with the former basis set is large. However, after using a larger basis set 6–311+G(3df), we have reached a excellent prediction of D_o for AgS and AuS within a very small error. Based on these facts, BPW91 method was chosen to optimize the structures and the succeeding CCSD(T) single-point calculations with 6–311+G(3df) basis set were carried out to obtain more accurate energies.

3.2. Reaction of Ag with CS_2

The doublet and quartet PESs of the reaction have been explored and two possible pathways are identified. Since the present studied species are open-shell system, we have to consider the reliabilities of current single-reference theoretical scheme. As shown in Table 5, the expectation value of $\langle S^2 \rangle$ for all doublet and quartet species indicate negligible spin contamination. In addition, the CCSD(T) T1 diagnostics [35], for which

Table 2
Total Energies (after zero-point energy correction, in a.u.), ZPE, relative energies (kcal/mol), the squared-magnitude of the total spin, and T1 diagnostic of the species in the reaction of Ag + CS_2

Species	UBPW91/BI				UCCSD(T)/BII//UBPW91/BI			
	Total energy	ZPE	Relative energy	$\langle S^2 \rangle$	Total energy	Relative energy[a]	$\langle S^2 \rangle$	T1[b]
^{2}Ag	−145.79636	0.0	–	0.751	−145.19634	–	0.751	0.006
^{4}Ag	−145.50423	0.0	–	3.751	−144.93792	–	3.752	0.005
^{2}AgS	−544.00187	0.00071	–	0.755	−542.92147	–	0.765	0.016
^{4}AgS	−543.93092	0.00034	–	3.754	−542.84499	–	3.766	0.018
CS($^1\Sigma_g$)	−436.24094	0.00286	–	0.0	−435.68506	–	0.000	0.026
^{1}CS$_2$($^1\Sigma^+$)	−834.54607	0.00676	–	0.0	−833.49171	–	0.000	0.021
^{3}CS$_2$(^{3}B$_2$)	−834.44723	0.00497	–	2.003	−833.39024	–	2.009	0.032
^{2}Ag + CS$_2$	−980.34243	0.00676	0.0	–	−978.68805	0.0	–	–
^{2}TS1(^{2}A′)	−980.33705	0.00605	3.4	0.752	−978.68626	1.1	0.757	0.018
^{2}Ag–η^1c(^{2}A$_1$)	−980.33728	0.00631	3.2	0.752	−978.68680	0.8	0.782	0.052
^{2}TS2(^{2}A)	−980.25458	0.00430	55.1	0.763	−978.62043	41.3	0.898	0.031
^{2}SAgCS($^2\Pi$)	−980.29693	0.00581	28.6	0.765	−978.66547	14.2	0.774	0.023
^{1}CS + ^{2}AgS	−980.24281	0.00357	62.5	–	−978.60653	51.2	–	–
^{2}Ag–η^1s(^{2}A′)	−980.34622	0.00684	−2.4	0.752	−978.69402	−3.7	0.787	0.020
^{4}Ag + CS$_2$	−980.05030	0.00676	183.3	–	−978.42963	162.2	–	–
^{2}Ag + ^{3}CS$_2$	−980.24359	0.00497	62.0	–	−978.58658	63.7	–	–
^{4}*iso*-Ag–η^1c(^{4}A)	−980.25289	0.00554	56.2	3.755	−978.59849	55.1	3.803	0.050
^{4}Ag–η^1c(^{4}B$_2$)	−980.24248	0.00734	62.7	3.754	−978.59502	58.4	3.789	0.027
^{4}TS2(^{4}A)	−980.20877	0.00446	83.9	3.758	−978.56388	76.8	3.843	0.040
^{4}SAgCS(^{4}A″)	−980.22307	0.00470	74.9	3.757	−978.58095	66.4	3.879	0.036
^{4}Ag–η^1s(^{4}A)	−980.24989	0.00551	58.1	3.756	−978.59149	60.6	3.798	0.035
^{4}AgS + CS	−980.17186	0.00320	107.0	–	−978.52879	99.9	–	–

[a] The total energies include ZPE obtained at the UBPW91/BI level.
[b] T1 diagnostic from CCSD(T) calculations.

Table 3
Total energies (after zero-point energy correction, in a.u.), ZPE, relative energies (kcal/mol), and the squared-magnitude of the total spin, and T1 diagnostic of the species in the reaction of $Au + CS_2$

Species	UBPW91/BI				UCCSD(T)/BII//UBPW91/BI			
	Total energy	ZPE	Relative energy	$\langle S^2\rangle$	Total energy	Relative energy	$\langle S^2\rangle$	T1
^{2}Au	−135.49393	0.0	–	0.752	−134.81156	–	0.752	0.008
^{4}Au	−135.24541	0.0	–	3.751	−134.59709	–	3.750	0.006
^{2}AuS	−533.71451	0.00084	–	0.753	−532.55103	–	0.767	0.026
^{4}AuS	−533.66610	0.00067	–	3.756	−532.49603	–	3.784	0.033
$^2Au + CS_2$	−970.04000	0.00676	0.000	0.0	−968.30327	0.0	–	–
^2Au–η^1s(^{2}A′)	−970.05483	0.00702	−9.3	0.75	−968.32222	−11.9	0.833	0.023
^{2}TS3(^{2}A′)	−970.04301	0.00627	−1.9	0.753	−968.31888	−9.8	0.794	0.023
^2Au–η^2cs(^{2}A′)	−970.04721	0.00664	−4.5	0.754	−968.32334	−12.6	0.811	0.029
^{2}TS4(^{2}A)	−969.96361	0.00451	47.9	0.759	−968.24587	36.0	0.795	0.046
^{2}SAuCS($^2\Pi$)	−970.04397	0.00651	−2.5	0.756	−968.33311	−18.7	0.775	0.024
$CS + ^2$AuS	−969.95545	0.00371	53.0	–	−968.23608	42.2	–	–
^2Au–η^1c($^2B_2$)	−970.03093	0.00672	5.7	0.758	−968.30192	0.8	0.876	0.047
$^4Au + {}^1CS_2$	−969.79148	0.00689	155.9	–	−968.08867	134.7	–	–
$^2Au + {}^3CS_2$	−969.91661	0.00497	77.4	–	−968.20180	63.7	–	—
^4Au–η^1s(^{4}A)	−969.96427	0.00578	47.5	3.755	−968.22710	47.8	3.812	0.034
^{4}TS3(^{4}A)	−969.95557	0.00509	53.0	3.755	−968.22514	49.0	3.820	0.031
^4Au–η^2cs(^{4}A)	−969.96526	0.00550	46.9	3.756	−968.23716	41.5	3.845	0.036
^{4}TS4(^{4}A)	−969.93540	0.00477	65.6	3.760	−968.21233	57.1	3.831	0.047
^{4}SAuCS(^{4}A)	−969.96963	0.00509	44.2	3.756	−968.25021	33.3	3.886	0.039
$CS + ^4$AuS	−969.90704	0.00353	83.4	–	−968.18109	76.7	–	–
^4Au–η^2ss(^{4}A)	−969.95726	0.00569	51.9	3.757	−968.23023	45.8	3.819	0.027

Table 4
Calculated vibrational frequencies (cm^{-1}) and IR intensities (km/mol, in parentheses) of the species in the present reaction

Species	Frequencies (IR intensity)
^{2}AgS($C_{\infty v}$)	312 (4)
^2Ag–η^1s(C_s)	40 (0), 101 (0), 347 (55), 375 (1), 635 (21), 1505 (539)
^2Ag–η^1c(C_{2v})	70 (1), 112 (9), 301 (227), 357 (9), 605 (178), 1326 (315)
^{2}SAgCS($C_{\infty v}$)	44 (1), 45 (0), 239 (6), 269 (8), 271 (2), 349 (5), 1334 (577)
^{2}TS1(C_s)	−152 (122), 61 (0), 210 (176), 360 (6), 610 (96), 1416 (345)
^{2}TS2(C_1)	−315 (17), 57 (3), 127 (12), 187 (1), 281 (6), 1237 (411)
^{4}*iso*-Ag–η^1c(C_1)	83 (0), 122 (2), 267 (11), 323 (8), 710 (183), 928 (9)
^{4}SAgCS(C_s)	44 (0), 45 (0), 158 (10), 273 (0), 402 (6), 1140 (1)
^4Ag–η^1c(C_{2v})	21 (1), 87 (1), 274 (2), 739 (0), 328 (11), 1167 (411)
^{4}TS2(C_1)	−75 (0), 126 (4), 142 (6), 194 (1), 328 (11), 1167 (411)
^{2}AuS($C_{\infty v}$)	371 (0)
^2Au–η^1c(C_{2v})	150 (6), 188 (4), 365 (10), 394 (12), 906 (223), 948 (20)
^2Au–η^1s(C_s)	65 (0), 187 (0), 343 (40), 366 (2), 629 (8), 1488 (512)
^2Au–η^2cs(C_s)	90 (3), 173 (1), 390 (6), 392 (90), 608 (95), 1260 (282)
^{2}SAuCS($C_{\infty v}$)	54 (0), 57 (0), 314 (2), 346 (5), 356 (0), 364 (9), 1368 (553)
^{2}TS3(C_s)	−189 (27), 120 (2), 190 (13), 373 (3), 617 (7), 1451 (420)
^{2}TS4(C_1)	−303 (38), 59 (4), 145 (7), 217 (1), 329 (3), 1229 (420)
^4Au–η^1s(C_1)	63 (0), 197 (3), 245 (6), 288 (9), 735 (7), 1009 (63)
^4Au–η^2cs(C_1)	34 (0), 134 (2), 202 (9), 412 (7), 687 (89), 884 (15)
^{4}SAuCS(C_1)	54 (0), 56 (1), 175 (7), 322 (0), 481 (3), 1134 (4)
^4Au–η^2ss(C_1)	125 (0), 126 (0), 186 (1), 323 (1), 712 (2), 1924 (58)
^{4}TS3(C_1)	−187 (1), 88 (0), 180 (2), 265 (2), 700 (3), 1001 (11)
^{4}TS4(C_1)	−107 (8), 141 (3), 181 (5), 193 (4), 412 (6), 1165 (426)
CS($C_{\infty v}$)	1257 (79)
$^1CS_2$($D_{\infty h}$)	384 (3), 384 (3), 658 (0), 1542 (525)
$^3CS_2$(C_{2v})	276 (0), 781 (2), 1039 (16)

values smaller than 0.02 usually accepted to support the validity of a single-determinant description of the reference wave functions, are also reported in Tables 2 and 3. For many of the doublet species, the T1 calculated values are indeed very close to the threshold of 0.02. But the diagnostic for some species are much greater than 0.02. The additional calculations show that for the most of these species have a dominant configuration with a weight of more than 95% and a second most important one having a participation of about 1–4.8%. Only the species ^2Ag–η^1c, ^{4}*iso*-Ag–η^1c, ^2Au–η^1c, and ^{4}TS4 have strong multi-reference characters. The result suggests that the present studied species are adequately described by the single-reference methods and the CCSD(T) calculated energies should be reliable.

Unless stated specifically, the energies of all species discussed in the following sections are obtained at the UCCSD(T) level including the ZPE corrections obtained with UBPW91 method.

In this section, we will discuss the doublet reaction pathway in details first, and then the quartet reaction pathway briefly.

3.2.1. *Doublet pathway of the reaction Ag + CS_2*

Previous theoretical investigations [18–20] indicate that the reactions of first-row transition-metal atoms with CS_2 can proceed through a similar insertion–elimination mechanism. An inserting-product SMCS is formed via different insertion pathways. In each pathway, a metal atom attracts a CS_2 molecule to form a complex. Then the complex is converted into an insertion product SMCS. As shown in Scheme 1, four insertion pathways are present and lead to four complexes. In this work, we firstly optimized the possible M–S coordinated complexes, and then tried to find the corresponding pathway. As shown in Fig. 3, two encounter complexes, ^2Ag–η^1s(C_s, ^{2}A′) and ^2Ag–η^1c(C_{2v}, $^2A_1$) have been located on the doublet PES. We tried to find other complexes ^2Ag–η^2cs and ^2Ag–η^2ss, but failed. The complex ^2Ag–η^1s have been reported previously [21]. The optimized structure by us is very close to that by Zeng et al. [21]. The

Table 5
Spin densities on atoms of all species at the UBPW91/BI level

Species	Ag + CS_2				Species	Au + CS_2			
	Ag	C	S1	S2		Au	C	S1	S2
^{2}Ag	1.00	–	–	–	^{2}Au	1.00	–	–	–
TS1	0.88	0.30	-0.09	−0.09	^{2}Au–η^1s	0.80	0.20	−0.21	0.21
^{2}Ag–η^1c	0.65	0.22	0.07	0.07	^{2}TS3	0.99	0.11	−0.26	0.16
^{2}TS2	0.04	0.06	0.83	0.07	^{2}Au–η^2cs	0.81	0.03	0.01	0.15
^{2}SAgCS	0.04	−0.07	1.04	−0.01	^{2}TS4	0.16	0.19	0.57	0.08
					^{2}SAuCS	0.00	−0.02	0.99	0.03
^{4}*iso*-Ag–η^1c	0.72	0.64	0.82	0.82	^{4}Au–η^1s	0.86	0.70	0.62	0.82
^{4}TS2	0.44	0.55	1.68	0.33	^{4}TS3	1.10	0.47	0.79	0.65
^{4}SAgCS	0.24	0.62	1.70	0.33	^{4}Au–η^2cs	0.98	0.33	0.86	0.84
					^{4}TS4	0.89	0.33	1.63	0.22
					^{4}SAuCS	0.37	0.53	1.60	0.50

^{2}Ag–η^1c complex is first reported by us. At last, we identified a doublet pathway (η^1c pathway), where the insertion reactions start from the M–η^1c complex. However, the reaction may proceed through a direct abstraction mechanism. Therefore, we attempted to locate the transition state of Ag–S–CS. But, no tight structure resulted from direct abstraction reaction has been found on the doublet and quartet PESs.

In the η^1c pathway, the reaction proceeds via two steps. Initially, the silver atom binds to the carbon atom of carbon disulfide molecule to form complex ^{2}Ag–η^1c, which is only 0.8 kcal/mol higher than the reactants (^{2}Ag + CS_2). The result indicates that a so-called entrance transition state [19,36] may exist and connect the reactants and the intermediate ^{2}Ag–η^1c on the doublet PES. In fact, we do find such a transition state ^{2}TS1. The transition state is 1.1 and 0.3 kcal/mol less stable than those of the reactants and the ^{2}Ag–η^1c intermediate. The C–S bond length in ^{2}Ag–η^1c is 1.610 Å, which is longer than the normal length 1.569 Å in CS_2 molecule. Thus, the C–S bond has been activated by silver atom at the initial step. The ^{2}Ag–η^1c is converted to an insertion product through a transition sate ^{2}TS2 with a very high activated barrier of 40.5 kcal/mol. The intermediate ^{2}Ag–η^1c and insertion product are connected by the transition state ^{2}TS2, which have been confirmed by IRC analysis. From ^{2}Ag–η^1c to ^{2}SAgCS through ^{2}TS2, the distance between Ag and S1 atoms decreases from 3.08 to 2.318 Å, whereas the C–S1 bond increases from 1.61 to 4.32 Å. In ^{2}SAgCS, the bond length of Ag–S1 is close to that in AgS. Thus, the bond C–S1 is completely broken and a new Ag–S bond is formed. In the C–S bond cleavage step from ^{2}Ag–η^1c to ^{2}SAgCS, the spin densities on the Ag an S1 atoms change from (0.65, 0.07) to (0.04, 1.04). The result suggests that an electron in Ag has been transferred to the S1 atom.

In the insertion product ^{2}SAgCS, the NBO charge on Ag atom is +0.6e. This species can be considered as a strongly bonded complex between two polar diatomic molecules, AgS and CS. NBO analysis also shows that triple and single bonds have been formed between atoms C and S2, and Ag and S1, respectively. The dissociation of ^{2}SAgCS into ^{2}AgS + CS is barrierless and the binding energy of SAg–CS is 37.0 kcal/mol. This value is smaller than those of STi–CS (46.8 kcal/mol) [19], SNi–CS (44.6 kcal/mol) [19], SV–CS (42.6 kcal/mol) [18], and SCu–CS (43.0 kcal/mol) [20] as reported in previous studies.

In conclusion, the overal reaction undergoes a C–S bond activation and cleavage step. And the later is the rate-determining step of the whole reaction.

Table 6
Natural charges on atoms of all species at the UBPW91/BI level

Species	Ag + CS_2				Species	Au + CS_2			
	Ag	C	S1	S2		Au	C	S1	S2
^{2}Ag	0.0	–	–	–	^{2}Au	0.0	–	–	–
CS_2		−0.44	0.22	0.22	^{2}Au–η^1s	0.01	−0.45	0.18	0.28
^{2}TS1	0.18	−0.57	0.19	0.20	^{2}TS3	0.03	−0.51	−0.21	0.28
^{2}Ag–η^1c	0.33	−0.65	0.16	0.16	^{2}Au–η^2cs	0.29	−0.65	0.16	0.17
^{2}TS2	0.76	−0.50	−0.55	0.29	^{2}TS4	0.71	−0.54	−0.48	0.31
^{2}SAgCS	0.61	−0.44	−0.49	0.32	^{2}SAuCS	0.53	−0.45	0.32	−0.41
^{2}Ag–η^1s	0.09	−0.45	0.13	0.22	^{2}AuS	0.35	–	−0.35	–
^{4}*iso*-Ag–η^1c	0.33	−0.79	0.23	0.23	^{4}Au–η^1s	0.07	−0.52	0.18	0.27
^{4}TS2	0.52	−0.58	−0.15	0.21	^{4}TS3	0.07	−0.56	0.21	0.28
^{4}SAgCS	0.59	−0.63	−0.11	0.15	^{4}Au–η^2cs	0.31	−0.79	0.24	0.25
					^{4}TS4	0.41	−0.55	−0.10	0.25
					^{4}SAuCS	0.51	−0.61	−0.09	0.20

The thermal enthalpies at 298 K for the reactants and insertion product ^{2}SAgCS have been calculated. As a result, the whole process is endothermic by about 21.0 kcal/mol, which is in good agreement with Zeng's work [21].

3.2.2. Quartet pathway of the reaction Ag + CS_2

The quartet ^{4}Ag state is about 162 kcal/mol above the doublet ^{2}Ag state. The ^{2}Ag atom may interact with a triplet $^3CS_2$ to form a ^{4}A surface, which is 64 kcal/mol higher than the ground-state reactants (^{2}Ag + CS_2). The quartet PES is much higher than the doublet PES. But in the doublet pathway, some species have very high energies. For example, ^{2}TS2 is 41.3 kcal/mol higher than the ground-state reactants. Furthermore, since the reaction proceeds under condition of photolysis, we have to consider the possible quartet pathway.

The potential energy profile of a quartet is somewhat different from that of a doublet. At the initial step of the reaction, Ag atom is added to the triplet $^3CS_2$ without entrance barrier to form a pyramidal complex *iso*-^{4}Ag–η^1c. Another planar η^1c complex ^{4}Ag–η^1c with C_{2v} symmetry has also been located. But its energy is 3.3 kcal/mol higher than that of the *iso*-^{4}Ag–η^1c. The transformation of the complex *iso*-^{4}Ag–η^1c to a bend insertion product ^{4}SAgCS yields through a transition state ^{4}TS2 with a barrier of 15.6 kcal/mol. IRC calculations confirm that the intermediate *iso*-^{4}Ag–η^1c and insertion product are connected by ^{4}TS2. The structure of ^{4}TS2 is similar to that of ^{2}TS2. But it lies above the ground-state reactants by 76.8 kcal/mol.

From Fig. 1, one can see that the quartet PES is always higher than the doublet PES. In experiment research, the insertion product SAgCS yields under photolysis. However, since energies of the species on quartet PES are significantly higher than those on doublet PES, the reaction is more likely to proceed through the doublet pathway. Intersystem crossing between the two PESs is unlikely to occur.

3.3. Reaction of Au with CS_2

3.3.1. Doublet pathway of the reaction Au + CS_2

On the doublet PES, three M–S coordinated complexes ^{2}Au–η^1s(C_s, ^{2}A′), ^{2}Au–η^2cs(C_s, ^{2}A′) and ^{2}Au–η^1c(C_{2v}, $^2B_2$) have been located and a η^1s pathway has been identified, which proceeds through the formation of intermediate complexes ^{2}Au–η^1s and ^{2}Au–η^2cs. The ^{2}Au–η^1c is 0.8 kcal/mol less stable than the reactants. No pathway leading to its formation has been found.

At the initial step of the pathway, an Au atom collides with the CS_2 molecule to form a complex ^{2}Au–η^1s with binding energy of 11.9 kcal/mol. The ^{2}Au–η^1s overpasses a planar transition state ^{2}TS3 with a small barrier of 2.1 kcal/mol, and is converted to a C–S bridged intermediate ^{2}Au–η^2cs, which lies below the ground reactants (^{2}Au + $^1CS_2$) by 12.6 kcal/mol. In this step, the two intermediate complexes and transition state have lower energy than the reactants. Hence this step is easy to proceed. In this stage, the C–S1 bond length gradually increases from 1.569 Å in CS_2 to 1.589 Å in ^{2}Au–η^1s and 1.604 Å in ^{2}TS3, then 1.646 Å in ^{2}Au–η^2cs. The results reveal that the C–S1 bond is activated. In the next insertion step, the insertion product ^{2}SAuCS is formed to complete the reaction via an insertion transition state ^{2}TS4 with a very high barrier of 48.6 kcal/mol. From the intermediate ^{2}Au–η^2cs to the insertion product ^{2}SAuCS, the C–S1 distance elongates from 1.646 to 4.171 Å and the Ag–S1 distance contracts from 2.745 to 2.262 Å. The Ag–S1 bond length of ^{2}SAuCS (2.262 Å) is close to that of the diatomic AuS (2.228 Å). Thus, a new Ag–S bond forms and the bond C–S1 is completely broken. In the C–S bond cleavage step, the spin densities on the Au an S1 atoms vary from (0.81, 0.01) to (0.0, 0.99). The result indicates that an electron of Au has been transferred to the S1 atom. The dissociation of ^{2}SAuCS into ^{2}AuS + CS is also barrierless but the binding energy of SAu–CS is 42.2 kcal/mol. NBO calculations show that there is a one-electron bond between Au and C.

From the reactants to ^{2}SAuCS, the reaction starts from the formation of an "end-on" complex ^{2}Au–η^1s and goes through a "side-on" complex ^{2}Au–η^2cs to reach the insertion product by a very high barrier. The insertion step is the rate-limiting step in the whole process. The pathway is similar to an energy favorable pathway of the reaction Cu + CS_2. The whole reaction is slightly exothermic by about 8.8 kcal/mol at 298 K. However, the result is different from the previous theoretical prediction by Zeng et al. [21]. After calculating the energy of the reactant (Au + CS_2) and product (SAuCS) at the B3LYP level of theory, they deduced that the reaction is endothermic by about 7.8 kcal/mol. We also optimized the reactant and product at the B3LYP level of theory. The calculated value is same to Zeng's result [21]. However, after performed single-point energy calculation at the CCSD(T) level of theory with B3LYP optimized structure, we found that the energy of product is 5.5 kcal/mol lower than it of reactant. Considering the reliability of CCSD(T) method, we think the reaction is slightly exothermic.

3.3.2. Quartet pathway of the reaction Au + CS_2

As seen from Fig. 4, the atoms of the species on doublet PES are almost in a plane. But the quartet structures are not planar. The quartet pathway also undergoes through the "end-on" and "side-on" complexes. But the two potential energy diagrams are different. In the quartet pathway, the Au atom interacts with the triplet $^3CS_2$ to form an "end-on" complex ^{4}Au–η^1s, which then transforms to a "side-on" complex ^{4}Au–η^2cs through the transition state ^{4}TS3 with a small barrier of 1.2 kcal/mol. The bend insertion product ^{4}SAuCS is formed through an insertion transition state ^{4}TS4 with a barrier of 15.7 kcal/mol. The ^{4}TS4 lies above the ground-state reactants Au and $^1CS_2$ by 57.1 kcal/mol.

From Fig. 2, one can see that the quartet PES is also higher than the doublet one. Intercrossing between the two PESs cannot occur so that the reaction would go along the doublet pathway.

3.4. Comparisons with experimental results and related theoretical studies

In experimental investigation on the two present reactions [21], the infrared spectra were reported and the assignment of the infrared absorptions was supported by B3LYP calculations. The IR bands observed and calculated by Zeng et al. [21] are listed in Table 7, along with calculated values in this work. As

Table 7
Comparison of observed and calculated vibrational frequencies (cm^{-1})

Species	υ		
	Observed, Ref. [21]	Calculated, Ref. [21]	Calculated, this work
^{2}Ag–η^1s	1507.1	1537.7	1505
^{2}SAgCS	1362.2	1373.4	1334
^{2}Au–η^1s	1485.9	1519.9	1488
^{2}SAuCS	1382.2	1407.6	1368

one can see, our calculated vibrational frequencies are very close to the experimental values. The good agreement indicates that BPW91 method is reliable and is very good for the calculation of small molecules containing Ag and Au.

Our proposed mechanisms show that the reaction $Ag + CS_2$ proceeds through an intermediate coordination complex ^{2}Ag–η^1c. However, in the experiment study on the reaction [21], only the Ag–η^1s complex has been detected. Thus, Zeng et al. [21] concluded that the reaction starts from the Ag–η^1s complex. The present result is contrary to the previous experiment observation.

The experiment fact that the coordination complex ^{2}Au–η^1s can be formed on annealing (without activation energy) is verified by our calculations. The insertion products SAgCS and SAuCS were only observed on broadband photolysis. Zeng et al. [21] suggested that the two reactions required activation energy. Our theoretical results show that the formations of the two insertion products need to overpass activation barriers of about 40 kcal/mol with respect to the ground-state reactants. Hence the mechanisms we proposed for the studied reactions are in energetic consistent with the experimental facts. The present study provides a reasonable explanation to the experimental observations.

In the previous investigation on the reaction $V^+ + CS_2$ [8], triplet and quintet PESs were explored. The theoretical study reveals that the formation of the lower-spin (triplet) ground state of product from high-spin (quintet) ground states of the reactant requires a spin inversion. The spin-orbital effects result in the occurrence of surface crossing. This process is a typical example of two-states of reactivity (TSR) [37]. In the present studied reactions, the quartet PES remains above that of the reactant ground states throughout the entire reaction path. The spin inversion is not required to form the final product. On the other hand, the doublet PES is much lower than the quartet PES. The energy difference between the corresponding species is quite large. Compared the large energy gap, the spin-orbital coupling effect is relatively small, unable to alter the reaction mechanism.

In the previous theoretical works, the reaction mechanism between first-row transition-metal atoms, Ti($3d^24s^2$) [19], V($3d^34s^2$) [18], Ni($3d^94s^1$) [19], Cu($3d^{10}4s^1$) [20] and CS_2 have been studied with DFT methods. It is very interesting to compare mechanisms and reactivities of the first-row transition-metal atoms with those of the second and third row transition-metal atoms, Ag and Au. The proposed mechanism for reactions $Ag + CS_2$ and $Au + CS_2$ is an insertion–elimination mechanism, which is similar to those of the first-row transition-metal atoms. Among these atoms, the Ti($3d^24s^2$) and V($3d^34s^2$) are very reactive with CS_2. The two reactions are exothermic and require no activation barriers [18,19]. For Ni atom, two triplet and one singlet pathways have been identified. Intercrossing between the two PESs may occur [19]. The reaction undergoes preferentially on triplet surface with a positive reaction energy barriers of 7 kcal/mol. Dobrogorskaya et al. [20] have explored the $^2Cu + CS_2$ reaction using DFT and CCSD(T) methods. The calculations indicated that copper atom is less active than the other first-row transition atoms to react with CS_2. To form the insertion product, the reaction has to overcome an energy barrier of at least 26 kcal/mol with respect to the ground-state reactants. Compared with the first-row transition atoms, silver and gold atoms are much less reactive. The two studied reactions have comparable energy barriers of about 40 kcal/mol. But the copper atom is more active than the other two coinage metals. Cu, Ag, and Au atoms have the same $(n-1)d^{10}ns^1$ electronic configuration, whereas all the three insertion reactions can be obtained only after photolysis. The main reason for accounting for poor reactivity may be that the *d* electron of the coinage metal is difficult to be back-donated into the π^* orbital of the C–S bond from the fully filled *d* electron shell. As a result, the coordination between the coinage metal and CS_2 is very weak and the C–S bond activation by the metal atoms is not very effective.

To conclude, the reaction mechanisms of $M + CS_2 \rightarrow MS + CS$ (M = Ag and Au) are similar to the previous reported one for the first-row transition-metal atoms with CS_2. But the reactivities of Ag and Au atom are lower than those of first-row transition-metal atoms.

4. Conclusion

The reaction mechanisms of Ag and Au atom toward CS_2 on doublet and quartet surfaces have been studied using UBPW91 and UCCSD(T) methods. One doublet and one quartet pathway are found for each reaction. The quartet PES is always much higher than the doublet PES. Intersystem crossing between the two PESs is unlikely to occur. The reaction is more likely to proceed through the doublet pathway. The doublet reaction route on PES leads to an insertion product SAgCS through the formation of the complexes ^{2}Ag–η^1c. For the reaction $Au + CS_2$, the formation of complexes ^{2}Au–η^1s and ^{2}Au–η^2cs leads to the insertion product SAuCS. The former reaction is endothermic by about 21.0 kcal/mol. And the later is slightly exothermic by about 8.8 kcal/mol. Our calculated vibrational frequencies are in good agreement with the experimental values. The experimental fact that the insertion product SAgCS and SAuCS were only observed on broadband photolysis is in line with our theoretical calculations. Compared with the reactions of first-row transition-metal atoms with CS_2, the studied reactions undergo via a similar insertion–elimination mechanism but the reactivities of two reactions are much lower because they have to overpass a high energy barrier of about 40 kcal/mol. The present theoretical study provides a detailed picture of the C–S bond activation and cleavage in carbon disulfide mediated by coning atom Ag and Au.

Acknowledgements

This project is supported by the National Science Foundation of China (Grant no. 20503018) and the Strategic Grant from City University of Hong Kong (account no. 7001974). We are grateful to the referees for their constructive comments and suggestions concerning our original manuscript.

References

[1] E.I. Stiefel, in: E.I. Stiefel, K. Matsumoto (Eds.), Transition Metal Sulfur Chemistry, ACS Symposium Series 653, American Chemical Society, Washington, DC, 1996, p. 2, and references therein.
[2] T. Kondo, T. Mitsudo, Chem. Rev. 100 (2000) 3205.
[3] R.H. Holm, P. Kennepohl, E.I. Solomon, Chem. Rev. 96 (1996) 2239.
[4] W. Kaim, B. Schwederski, Bioinorganic Chemistry: Inorganic Elements in the Chemistry of Life, John Wiley & Sons, New York, 1994.
[5] M.J. Almond, B. Cockayne, S.A. Cooke, D.A. Rice, P.C. Smith, P.J. Wright, J. Mater. Chem. 6 (1996) 1639.
[6] I. Kretzschmar, D. Schröder, H. Schwarz, C. Rue, P.B. Armentrout, J. Phys. Chem. A 104 (2000) 5046.
[7] I. Kretzschmar, D. Schröder, H. Schwarz, C. Rue, P.B. Armentrout, J. Phys. Chem. A 102 (1998) 10060.
[8] C. Rue, P.B. Armentrout, I. Kretzschmar, D. Schröder, J.N. Harvey, H. Schwarz, J. Chem. Phys. 110 (1999) 7858.
[9] I. Kretzschmar, D. Schröder, H. Schwarz, C. Rue, P.B. Armentrout, Int. J. Mass Spectrom. 228 (2003) 439.
[10] C. Rue, P.B. Armentrout, I. Kretzschmar, D. Schröder, H. Schwarz, Int. J. Mass Spectrom. 210–211 (2001) 283.
[11] C. Rue, P.B. Armentrout, I. Kretzschmar, D. Schröder, H. Schwarz, J. Phys. Chem. A 105 (2001) 8456.
[12] C. Rue, P.B. Armentrout, I. Kretzschmar, D. Schröder, H. Schwarz, J. Phys. Chem. A 106 (2002) 9788.
[13] I. Kretzschmar, D. Schröder, H. Schwarz, C. Rue, P.B. Armentrout, Int. J. Mass Spectrom. 249–250 (2006) 263.
[14] P. Cheng, G.K. Koyanagi, D.K. Böhme, J. Phys. Chem. A 110 (2006) 2718.
[15] N. Jiang, D.J. Zhang, Chem. Phys. Lett. 366 (2002) 253.
[16] M.F. Zhou, L. Andrews, J. Phys. Chem. A 104 (2000) 4394.
[17] A.B. Baker, L. Andrews, J. Phys. Chem. A 110 (2006) 10419.
[18] I. Pápai, Y. Hannachi, S. Gwizdala, J. Mascetti, J. Phys. Chem. A 106 (2002) 4181.
[19] T.H. Li, X.G. Xie, S.L. Gao, C.M. Wang, W.X. Cheng, X.L. Pan, H. Cao, J. Mol. Struct. (THEOCHEM) 724 (2005) 125.
[20] Y. Dobrogorskaya, L. Mascetti, I. Pápai, A. Nemukhin, Y. Hannachi, J. Phys. Chem. A 107 (2003) 2711.
[21] A.H. Zeng, Q.Y. Kong, Y. Wang, M.F. Zhou, Chem. Phys. 292 (2003) 111.
[22] A.D. Becke, Phys. Rev. A 38 (1988) 3098.
[23] J.P. Perdew, K. Burke, Y. Wang, Phys. Rev. B 54 (1996) 16533.
[24] P.J. Hay, W.R. Wadt, J. Chem. Phys. 82 (1985) 299.
[25] A.W. Ehlers, M. Bohme, S. Dapprich, A. Gobbi, A. Höllwarth, V. Jonas, K.F. Köhler, R. Stegmann, A. Veldkamp, G. Frenking, Chem. Phys. Lett. 208 (1993) 111.
[26] M. Couty, M.B. Hall, J. Comput. Chem. 17 (1996) 1359.
[27] C. Gonzalez, H.B. Schlegel, J. Chem. Phys. 90 (1989) 2154.
[28] A.E. Reed, L.A. Curtiss, F. Weinhold, Chem. Rev. 88 (1988) 899.
[29] M.J. Frisch, G.W. Trucks, H.B. Schlegel, G.E. Scuseria, M.A. Robb, J.R. Cheeseman, J.A. Montgomery Jr., T. Vreven, K.N. Kudin, J.C. Burant, J.M. Millam, S.S. Iyengar, J. Tomasi, V. Barone, B. Mennucci, M. Cossi, G. Scalmani, N. Rega, G.A. Petersson, H. Nakatsuji, M. Hada, M. Ehara, K. Toyota, R. Fukuda, J. Hasegawa, M. Ishida, T. Nakajima, Y. Honda, O. Kitao, H. Nakai, M. Klene, X. Li, J.E. Knox, H.P. Hratchian, J.B. Cross, V. Bakken, C. Adamo, J. Jaramillo, R. Gomperts, R.E. Stratmann, O. Yazyev, A.J. Austin, R. Cammi, C. Pomelli, J.W. Ochterski, P.Y. Ayala, K. Morokuma, G.A. Voth, P. Salvador, J.J. Dannenberg, V.G. Zakrzewski, S. Dapprich, A.D. Daniels, M.C. Strain, O. Farkas, D.K. Malick, A.D. Rabuck, K. Raghavachari, J.B. Foresman, J.V. Ortiz, Q. Cui, A.G. Baboul, S. Clifford, J. Cioslowski, B.B. Stefanov, G. Liu, A. Liashenko, P. Piskorz, I. Komaromi, R.L. Martin, D.J. Fox, T. Keith, M.A. Al-Laham, C.Y. Peng, A. Nanayakkara, M. Challacombe, P.M.W. Gill, B. Johnson, W. Chen, M.W. Wong, C. Gonzalez, J.A. Pople, Gaussian 03 Revision D.01, Gaussian Inc., Wallingford, CT, 2004.
[30] S.Q. Niu, M.B. Hall, Chem. Rev. 100 (2000) 353.
[31] P.E.M. Siegbahn, M.R.A. Blomberg, Chem. Rev. 100 (2000) 421.
[32] F.S. Legge, G.L. Nyberg, J.B. Peel, J. Phys. Chem. A 105 (2001) 7905.
[33] P. Pyykkö, Angew. Chem. Int. Ed. 43 (2004) 4412.
[34] K.P. Huber, G. Herzberg, Molecular Spectra and Molecular Structure. IV. Constants of Diatonic Molecules, Van Nostrand Reinhold Company, New York, 1979.
[35] T.J. Lee, P.R. Taylor, Int. J. Quantum Chem. Symp. 23 (1989) 199.
[36] I. Pápai, G. Schubert, Y. Hannachi, J. Mascetti, J. Phys. Chem. A 106 (2002) 9551.
[37] D. Schröder, S. Shaik, H. Schwarz, Acc. Chem. Res. 33 (2000) 139.
[38] I. Suzuki, Bull. Chem. Soc. Jpn. 48 (1975) 1685.
[39] M.W. Chase Jr., C.A. Davies, J.R. Downey Jr., D.J. Frurip, R.A. McDonald, A.N. Syverud, J. Phys. Chem. Ref. Data 14 (Suppl. 1) (1985).